

One-loop Type II Seesaw Neutrino Model with Stable Dark Matter Candidates

M. A. Loualidi^{*§} and M. Miskaoui^{†§}

LPHE-Modeling and Simulations, Faculty of Sciences, Mohammed V University,
Rabat, Morocco

Abstract

Opening up the Weinberg operator at 1-loop level using a scalar triplet, two scalar doublets and one fermion gives rise to T4-2-i one-loop topology. Neutrino masses generated from this topology are always accompanied by the tree level Type II seesaw contribution. In this work, we propose a radiative Majorana neutrino mass model based on this topology where to avoid the tree level Type II seesaw mechanism, we extend the model by a $G_f = \mathbb{D}_4 \times Z_3 \times Z_5 \times Z_2$ flavor symmetry and we promote the fermion inside the loop to three right-handed neutrinos. In this scenario, the tree level Dirac neutrino masses resulted from these right-handed neutrinos is also prevented by the G_f group. Moreover, in order for T4-2-i topology to fully function, the scalar sector is extended by two flavon fields where after G_f symmetry breaking, the model accounts successfully for the observed neutrino masses and mixing as well as allows for the existence of stable dark matter (DM) candidates. Indeed, all the particles running in the loop are potential dark matter candidates as their stability is guaranteed by the unbroken discrete group $Z_2 \in G_f$.

Key words: Neutrino masses and mixing, Flavor symmetries, Dark matter stability.

^{*}E-mail: mr.medamin@gmail.com

[†]E-mail: m.miskaoui@gmail.com

[§]Both authors contributed equally to this work.

1 Introduction

The developments in the field of neutrino physics in the past two decades have been undoubtedly impressive. Neutrinos which rarely interact with ordinary matter have been identified in the Standard Model (SM) as massless particles. However, many neutrino oscillation experiments performed in the past twenty years confirmed that neutrinos have nonzero masses, thus making these particles as the current best probe for new physics beyond the SM (BSM) [1, 2]. Another matter that requires going BSM and which has been explored at length in the literature is the existence of dark matter where amongst its known properties, an appropriate candidate must have zero electric charge, produce the correct relic abundance and must be stable over cosmological time scales [3]. This stability asserts the existence of a new kind of charge carried by the DM particle, and in model building, the stability is usually guaranteed by imposing new symmetries like Z_2 which is the most commonly used symmetry in the literature.

In recent years, there have been a growing interest in radiative neutrino mass models that provide an interconnection between the neutrino and the DM sectors. Indeed, these models predict neutrino masses at the loop level as well as the existence of DM candidates in the form of one of the intermediate particles running in the loop. One class of these models is the n -loop realizations of the well-known $d = 5$ Weinberg operator $O_5 = LLHH$ where L stands for the $SU(2)_L$ lepton doublets while H denotes the $SU(2)_L$ Higgs doublet of the SM¹. A popular one-loop realization of O_5 is the scotogenic model which extends the SM particle content by three right-handed neutrinos and an extra inert scalar doublet [5], while an exact Z_2 symmetry prevents the tree level Dirac masses for neutrinos as well as allowing for stable DM candidates. This model has been studied in detail using the same and in many times different set of particles inside the loop; see, for instance, Refs. [6–46]. The full possible one-loop diagrams induced from this operator can be found in [47] while a systematic study of two and three-loop realizations of O_5 is done in [48, 49] and [50], respectively. For a detailed review on radiative neutrino mass models and their classification see [51] and the references therein. To explain neutrino data along with providing a good DM candidate in the context of radiative models, the particle content and the gauge symmetry of the SM, $G_{SM} = SU(3)_C \times SU(2)_L \times U(1)_Y$, need to be extended. Actually, there are no restrictions concerning whether the extra symmetries should be Abelian or non-Abelian, discrete or continuous, simple or multiple. On the other hand, it is well-known that non-Abelian discrete groups are well justified by the large leptonic mixing angles measured by the oscillation experiments, and when radiative models are extended by a non-Abelian flavor symmetry, an interesting implication is that the stability of DM candidate may be ensured by one of the subgroups obtained after breaking the flavor symmetry, see for instance Refs. [52–62]. Therefore, non-Abelian flavor symmetries are an effective tool to address both neutrino and dark matter issues.

While most of the finite one-loop diagrams are studied extensively in model-building BSM,

¹For a systematic investigation of radiative Dirac neutrino mass models emerging from one-loop and two-loop topologies, see for instance [4] and references therein.

there is in particular one topology that have never been realized in a field theory; it is denoted by T4-2-i as illustrated in figure 1 [23,47]. This topology involves a scalar triplet T —with hypercharge $Y = 2$ —two extra inert scalars ϕ and ρ and one fermion ψ running in the loop. The Higgs triplet T couples to the SM Higgs doublet H through the interaction $HT^\dagger H$, and thus, it will always involves the usual tree level Type II seesaw² contribution to neutrino masses LTL that cannot be prevented by any additional $U(1)$ or Z_N symmetries [23,47]. The authors in reference [47] stated that to prevent the tree level contributions, two things are required: (i) Promoting the fermion ψ inside the loop to be Majorana fermion; and (ii) assuming that all couplings conserve lepton number.

In this paper, our purpose is to cure the difficulties encountered when building a field theory with topology T4-2-i. To achieve this, we propose a radiative Majorana neutrino mass model within an extension of the SM based on the $G_f = \mathbb{D}_4 \times Z_3 \times Z_5 \times Z_2$ flavor symmetry. Furthermore, as previously mentioned, in order to obtain neutrino masses and mixing consistent with the current neutrino data along with providing a stable DM candidate, the obvious implication is that we must extend the particle content of the SM as well. Therefore, we proceed with the first requirement in [47] and we promote the fermion inside the loop to three right-handed neutrino singlets N_k , while we discard the second one; which means that we do not assume that all couplings must conserve lepton number. The alternative for the second requirement—which ensures the suppression of the tree level Type II seesaw contribution to neutrino masses LTL —is fulfilled by the choice of the particle assignment under $Z_3 \times Z_5 \in G_f$. Actually, our $Z_3 \times Z_5$ charge assignments given in Tables 2 and 3 prevent the tree level Type II seesaw contribution as well as the tree level Dirac Yukawa coupling $y_{ij}\bar{L}_i\tilde{H}N_j$, and eventually, the Type I seesaw contribution to neutrino masses. Thus, the only possibility for neutrino mass generation in our model is at the loop level in the scotogenic fashion. However, the price to pay with the Z_3 charge assignments is that the two Yukawa couplings connecting N_k , L and the two inert scalars in the loop of topology T4-2-i carry non trivial Z_3 charge. Moreover, the usual vertex connecting two Higgs doublets with the scalar triplet T (upper vertex in figure 1) is also prevented by the Z_3 symmetry. To restore Z_3 invariance, we have enlarged the scalar sector by adding two flavon fields F and χ carrying quantum numbers under G_f ; thus, fixing the issues of topology T4-2-i. When the flavon F acquires its vacuum expectation value (VEV), the \mathbb{D}_4 group gets broken down to a subgroup Z'_2 leading to a neutrino mass matrix compatible with the well-known trimaximal mixing matrix [65–71]. We have studied numerically the phenomenology associated with neutrino sector in the normal mass hierarchy (NH) case. Finally, for the DM candidates, all the particles running in the loop—right-handed neutrino N_k and the scalars ρ and ϕ —are odd under the discrete group $Z_2 \in G_f$ whilst all SM particles are even. Therefore, the lightest odd particle will be stable and can play the role of the DM candidate. We have discussed the validity of DM candidates for two cases; (a) Fermionic DM candidate with N_3 being the lightest odd particle, and (b) Bosonic DM candidate with ρ being the lightest odd

²Dark matter and neutrino mass problems are also studied in models where neutrino masses are generated by the tree level TypeII seesaw model mechanism, see, for instance [63,64].

particle. On the other hand, although the Z'_2 subgroup of \mathbb{D}_4 is unbroken, it is not responsible for DM stability; however, there might be processes allowed by Z_2 but forbidden by Z'_2 since the residual symmetry that survives the G_f symmetry breaking is given by the group $Z'_2 \times Z_2$. Thus, we have checked the invariance of the various DM processes under Z_2 as well as Z'_2 .

The paper is organized as follows. In Sec. II we start by a general discussion on topology T4-2-i, then we present our field content and the solution to the problems of topology T4-2-i. In Sec. III we start by studying in details the neutrino sector and then describe the phenomenology associated with neutrino masses and mixing. In Sec. IV we discuss the dark matter sector where we comment briefly the cases of fermionic and bosonic DM candidates. In Sec. V, we give our conclusion. Finally, we add an Appendix which contains some useful tools on the dihedral \mathbb{D}_4 group.

2 Genuine one-loop Type II seesaw using G_f flavour symmetry

In this section, we first describe the particles involved in topology T4-2-i and all their possible charge assignments under the electroweak (EW) gauge group and we provide the necessary requirements to fix the issues associated with topology T4-2-i. Then, we present our scenario to account for this topology by implementing the G_f flavor symmetry accompanied with extra flavon fields.

2.1 One loop Type II seesaw topology

There are several approaches to generate neutrino masses beyond the SM, among which are the radiative models where neutrino masses arise at the loop level. These models are rather interesting because they not only account for the tiny neutrino masses naturally, but also provide a DM candidate given by one of the new fields running in the loop. One of the most effective ways to classify these models is through the topology of the loop diagrams which generate neutrino masses [47, 48, 51, 72, 73]. The majority of these models are the one-loop realizations of the well-known dimension-5 Weinberg operator $LLHH$. While most of the finite one-loop diagrams are studied extensively in building BSM physics models, there is in particular one topology that have never been realized in a field theory; it is denoted by T4-2-i as illustrated in Fig. 1. In this topology, there are four new particles compared to the SM; an $SU(2)_L$ scalar triplet with hypercharge $Y = 2$ which couples to the SM Higgs doublets H (bottom vertex), two scalars ϕ and ρ and one fermion ψ running in the loop. From this, we deduce five different field assignments leading to five different models generating neutrino masses at one-loop. These five possibilities are reported in Table 1 using $SU(2)_L$ representations to differentiate between different models

On the other hand, it was mentioned in Refs. [23, 47] that topology T4-2-i will always involves

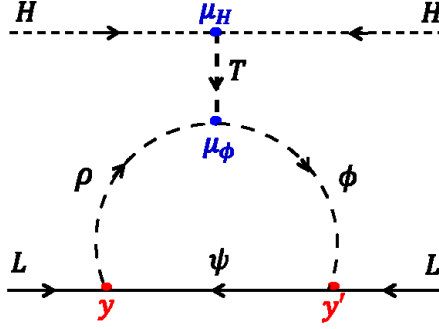


Figure 1: One-loop neutrino mass generation from an $SU(2)_L$ scalar triplet like in the Type II seesaw mechanism. This diagram is denoted as T4-2-i in reference [47].

Fields	Model I	Model II	Model III	Model IV	Model V
ϕ	3	2	2	1	3
ρ	1	2	2	3	3
ψ	2	1	3	2	2

Table 1: Different $SU(2)_L$ assignments for the fields ρ , ϕ and ψ leading to five possible one-loop neutrino mass models from topology T4-2-i.

the usual tree level Type II seesaw contribution to neutrino masses LTL that cannot be prevented by any additional $U(1)$ or Z_N symmetries. This can be easily shown by considering the hypercharge quantum numbers of the different particles involved in the tree level contribution as well as topology T4-2-i. Therefore, for the Type II seesaw mass term LTL we have the condition

$$2Y_L + Y_T = 0 \quad \text{with} \quad Y_L = -1 \text{ and } Y_T = 2, \quad (2.1)$$

where Y_X is the hypercharge of field X under the $U(1)_Y$ group. For topology T4-2-i, the loop in the diagram of Fig. 1 consists of three vertices with the following conditions on Y_X

$$\begin{aligned} Y_L - Y_\rho + Y_\psi &= 0 \quad \rightarrow \quad \text{vertex connecting } L, \phi \text{ and } \psi \\ Y_L + Y_\phi - Y_\psi &= 0 \quad \rightarrow \quad \text{vertex connecting } L, \rho \text{ and } \psi \\ Y_T + Y_\rho - Y_\phi &= 0 \quad \rightarrow \quad \text{vertex connecting } T, \phi \text{ and } \rho. \end{aligned} \quad (2.2)$$

The sum of these three equations leads to the condition (2.1) which implies that a neutrino mass generated by topology T4-2-i is always accompanied by the tree-level Type II seesaw mechanism. This is true for any $U(1)$ or Z_n quantum charges q_X . On the other hand, the authors in Refs. [23,47] stated that to prevent the tree level contributions, two things are required: (i) Promoting the fermion ψ inside the loop to be Majorana fermion; and (ii) assuming that all couplings conserve lepton number. In this regard, once these two conditions are imposed, the tree level Type II seesaw contribution LTL will be eliminated as it violates lepton number conservation while the Majorana mass term for the fermion running in the loop $M_i \bar{\psi}_i^c \psi_i$ will be the only term allowed to break lepton number. Moreover, these two conditions narrow down the number of $SU(2)_L \times U(1)_Y$

assignments for the fermion ψ to only two options: a fermion singlet or a fermion triplet both with hypercharge $Y = 0$. As a result, only the assignments in the models II and III from Table 1 are allowed in this scenario. However, building models and taking into account these prerequisites—especially the condition of imposing lepton number conservation—is not an easy task; thus, a call for additional symmetries and particles seems necessary. In this regard, we propose in the next subsection a solution to the issues of topology T4-2-i by extending the SM by a $\mathbb{D}_4 \times Z_3 \times Z_5 \times Z_2$ flavor symmetry.

2.2 Implementing G_f flavour symmetry in T4-2-i model

As mentioned above, the first step to forbid the tree level Type II seesaw coupling λLTL is by promoting the fermion ψ inside the loop to a Majorana fermion. In this work, we consider three right-handed neutrino singlets N_k which correspond to model II in Table (1). In a second step, we extend the SM gauge group with an additional $G_f = \mathbb{D}_4 \times Z_3 \times Z_5 \times Z_2$ flavor symmetry along with extra flavon fields allowing us to control the couplings in the 1-loop diagram. Actually, the choice of this additional symmetry in our model is introduced not only to forbid the tree level Type II seesaw contribution, but also to satisfy the following requirements: (i) forbid the tree level Type I seesaw contribution coming from the Dirac operator $y_{ij} \bar{L}_i \tilde{H} N_j$; (ii) obtain neutrino masses and mixing angles consistent with the current neutrino data; and (iii) stabilize the dark matter candidate against decay. Now we turn to present the particle content of the model and describe

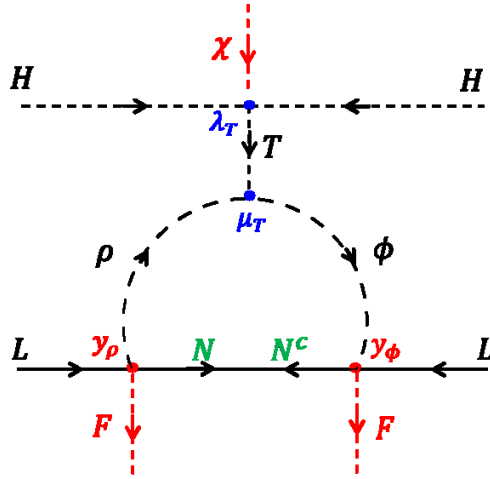


Figure 2: One-loop Feynman diagram responsible for the neutrino mass matrix in our $\mathbb{D}_4 \times Z_3 \times Z_5 \times Z_2$ model.

the G_f quantum numbers of the leptons as well as for new extra fields. Recall first that the discrete \mathbb{D}_4 group has five irreducible representations: four singlets $1_{p,q}$ with indices $p, q = \pm, \pm$; and one doublet 2 indexed by the characters $\chi(S)$, $\chi(T)$ of the two non-commuting generators S and T of the dihedral \mathbb{D}_4 ; see appendix for more details. For the lepton sector, as stated in the beginning of this subsection we have added three right-handed neutrinos to the usual $SU(2)$ lepton doublets L_i

and lepton singlets l_i^R of the SM, here i run over the three lepton families. Their quantum numbers under the SM gauge group and the G_f flavor group are as given in Table 2. For the scalar sector,

Fermions	L_e	L_μ	L_τ	l_e^R	l_μ^R	l_τ^R	N_1	N_2	N_3
G_{SM}	$(1, 2)_{-1}$			$(1, 1)_{-2}$			$(1, 1)_0$		
\mathbb{D}_4	$1_{+,+}$	$1_{+,-}$	$1_{-,+}$	$1_{+,+}$	$1_{+,-}$	$1_{-,+}$	$1_{+,+}$	$1_{+,-}$	$1_{-,+}$
(Z_3, Z_2)	$(1, 1)$			$(\omega, 1)$			$(1, -1)$		
Z_5	1			η^2			1		

Table 2: Gauge and flavor quantum numbers for leptons and right-handed neutrino fields, where $\omega = e^{\frac{2\pi i}{3}}$ and $\eta = e^{\frac{2\pi i}{5}}$.

besides the usual SM Higgs doublet $H = (h^+, h^0)$, the model involves five additional scalar fields; two inert Higgs doublets $\rho = (\rho^0, \rho^-)$ and $\phi = (\phi^+, \phi^0)$, one $SU(2)$ scalar triplet T and two flavon fields F and χ . In our model, the extra right-handed neutrinos N_k and the inert Higgs doublets

Scalars	H	T	ρ	ϕ	F	χ
G_{SM}	$(1, 2)_1$	$(1, 3)_2$	$(1, 2)_{-1}$	$(1, 2)_1$	$(1, 1)_0$	$(1, 1)_0$
\mathbb{D}_4	$1_{+,+}$	$1_{+,+}$	2	2	2	$1_{+,+}$
(Z_3, Z_2)	$(\omega^2, 1)$	$(\omega^2, 1)$	$(\omega^2, -1)$	$(\omega, -1)$	$(\omega, 1)$	$(\omega, 1)$
Z_5	η^3	1	1	1	1	η^4

Table 3: Gauge and flavor quantum numbers for all scalar fields of the model.

ρ and ϕ are running in the loop as in the original topology of Fig. 1. However, based on the G_f charge assignments shown in Table 3, the two Yukawa couplings $y_{ik}\bar{L}_i\rho N_k$ and $y'_{jk}\bar{L}_i\tilde{\phi}N_k$ behave as doublets under \mathbb{D}_4 group and they carry non zero Z_3 charge ω^2 . To restore the invariance under the $\mathbb{D}_4 \times Z_3$ symmetry, we have added the flavon field F which transforms as a \mathbb{D}_4 doublet and carries a Z_3 charge ω . On the other hand, the one-loop vertex $\mu_H HT^\dagger H$ connecting two Higgs doublets with the scalar triplet in Fig. 1 is prevented in our model by the Z_3 symmetry since its charge is ω^2 , the invariance is restored by the flavon field χ which carries the charge ω , see Table 3. The resulted couplings are invariant under the Z_2 symmetry which will be only used to stabilize the dark matter candidate. Moreover, to guarantee a genuine 1-loop neutrino mass model—no tree level contribution to neutrino masses—, the dimension-5 operator $L_i^T T L_j \chi$ which is allowed by the $\mathbb{D}_4 \times Z_3$ symmetry and leads to a Type II seesaw tree-level contribution is prevented by the discrete $Z_5 \in G_f$ symmetry under which this terms transform as η^4 ; see Tables 2 and 3 for the Z_5 quantum numbers of the matter and scalar fields respectively. Therefore, the $\mathbb{D}_4 \times Z_3 \times Z_5$

group and the new flavon fields are sufficient to address the challenge of Topology T4-2-i, leading subsequently to the modified one-loop radiative diagram shown in Fig. 2. In the following section, we will study in details the neutrino masses and mixing and their corresponding phenomenological consequences.

Before we describe the neutrino sector, let us comment briefly on the charged lepton masses. With respect to the chosen \mathbb{D}_4 particle assignments—see Tables 2 and 3—the charged lepton mass matrix is diagonal. This can easily be seen by considering the leading order terms responsible for the charged lepton masses. These terms invariant under G_f are $y_e (\bar{L}_e)_{++} (e_R)_{++} (H)_{++}$, $y_\mu (\bar{L}_\mu)_{+-} (\mu_R)_{+-} (H)_{++}$ and $y_\tau (\bar{L}_\tau)_{-+} (\tau_R)_{-+} (H)_{++}$. Therefore, after the Higgs field takes its VEV as $\langle H \rangle = \begin{pmatrix} 0 & \frac{1}{\sqrt{2}}(v_H + h + iA) \end{pmatrix}^T$, we obtain a diagonal charged lepton mass matrix as $m_l = v_H/\sqrt{2} \text{diag}(y_e, y_\mu, y_\tau)$. However, it is clear that it is not trivial to produce the mass hierarchy among charged leptons at the leading order where we need to impose a hierarchical values on the Yukawa couplings, which is considered very unnatural. On the other hand, in flavor symmetries based models, the mass hierarchy can be achieved by taking into account corrections in the the charged lepton mass matrix from higher-dimensional operators involving flavon fields. An example of such operators can be written as $\bar{L}_l^i l_R^j H (\frac{\Omega}{\Lambda})^n (\frac{\zeta}{\Lambda})^m$ with $n + m \geq 1$ and Λ is a cutoff scale while Ω and ζ denote the flavon fields needed also to ensure the invariance under G_f . Another attractive method used to explain this hierarchy is the Froggatt-Nielsen mechanism which relies on the spontaneous breaking of a $U(1)_F$ flavor symmetry, for details on this method see Ref. [74].

3 Neutrino model building based on topology T4-2-i

In this section, we study the neutrino masses and mixing in the framework described in the previous subsection. Neutrino masses are generated radiatively while we considered the trimaximal mixing matrix scheme. Then, by using the 3σ experimental values of the oscillation parameters, we show by means of scatter plots the physical observables m_{ee} and m_{ν_e} related respectively to neutrinoless double beta decay and tritium beta decay experiments, and we also provide scatter plot predictions on the sum of neutrino masses as well as on the Dirac CP violating phase.

3.1 Neutrino masses and mixing

In our model, the G_f flavor symmetry forbids the usual SM tree level Dirac term $y \bar{L}_i \tilde{H} N_k$, and since the neutral component of the scalar fields ρ and ϕ do not acquire VEVs, the usual seesaw mechanism is no longer responsible for neutrino masses. Nonetheless, the light neutrino masses are generated radiatively through the one-loop diagram which involves ρ , ϕ and N_k in the internal lines; see Fig. 2. According to the field assignments in Tables 2 and 3, the relevant couplings in the neutrino sector, invariant under gauge and $\mathbb{D}_4 \times Z_3 \times Z_5 \times Z_2$ symmetries are given by the

following lagrangian

$$\mathcal{L} = \frac{y_\rho^{ik}}{\Lambda} \bar{L}_i N_k \rho F + \frac{y_\phi^{jk}}{\Lambda} \bar{L}_j N_k \tilde{\phi} F + \frac{M_k}{2} \overline{N_k^c} N_k + h.c., \quad (3.1)$$

Here y_ρ^{ik} and y_ϕ^{jk} are Yukawa couplings and $\tilde{\phi} = i\sigma_2 \phi^*$. The first two terms in this lagrangian are the leading order contributions to Dirac neutrino masses while the third one is the Majorana mass term for N_k . For example, the first coupling transforms under the \mathbb{D}_4 discrete symmetry as

$$\bar{L}_i N_k \rho F \sim 1_{a,b} \otimes 1_{c,d} \otimes 2 \otimes 2, \quad (3.2)$$

with indices $a, b, c, d = \pm$. Thus, to obtain the desired \mathbb{D}_4 trivial singlet, the tensor product between the \mathbb{D}_4 doublets—which decomposes into the direct sum of the four \mathbb{D}_4 singlets; see the Appendix—should transform in the same manner as the product between the two singlet $1_{a,b} \otimes 1_{c,d}$. This can easily be seen in the following examples

$$\begin{aligned} \bar{L}_e N_1 \rho F &\sim (1_{+,+} \otimes 1_{+,+})|_{1_{+,+}} \otimes (2 \otimes 2)|_{1_{+,+}} \\ \bar{L}_e N_2 \rho F &\sim (1_{+,+} \otimes 1_{+,-})|_{1_{+,-}} \otimes (2 \otimes 2)|_{1_{+,-}}. \end{aligned} \quad (3.3)$$

The same discussion holds for the second term in (3.1). To break the flavor symmetry, the flavon doublet F acquires its VEV along the direction $\langle F \rangle = v_F (1, 1)$ while the scalar fields ρ and ϕ do not acquire VEVs and may be expressed as

$$\rho = \begin{pmatrix} \frac{1}{\sqrt{2}}(\rho_1 + i\rho_2) \\ \rho^- \end{pmatrix}, \quad \phi = \begin{pmatrix} \phi^+ \\ \frac{1}{\sqrt{2}}(\phi_1 + i\phi_2) \end{pmatrix}, \quad (3.4)$$

with ρ_1 (ϕ_1) and ρ_2 (ϕ_2) present respectively the scalar and the pseudoscalar parts of the neutral component of ρ (ϕ). At the first sight, it seems that ρ and ϕ are adjoint of each other as they carry the hypercharges $Y = -1$ and $Y = +1$ and Z_3 charges $\bar{\omega}$ and ω respectively. However, they transform in the following manner under \mathbb{D}_4

$$\hat{\rho} = \begin{pmatrix} \rho \\ 0 \end{pmatrix} \quad \text{and} \quad \hat{\phi} = \begin{pmatrix} \phi \\ 0 \end{pmatrix} \quad (3.5)$$

in such a way that ρ and ϕ^\dagger are placed in different \mathbb{D}_4 doublet components; see Appendix for more details on \mathbb{D}_4 group properties. This difference between ρ and ϕ^\dagger is due to the vertex connecting T , ϕ and ρ in the diagram of Fig. 2, where by asking for a non-vanishing coupling $\mu_T T \rho \phi^\dagger$ the bilinear term ($\rho \phi^\dagger$) must transform as a trivial singlet (since $T \sim 1_{++}$). Using the \mathbb{D}_4 tensor product, the product between the two mass matrices deduced from the two first terms in (3.2) is given by

$$\frac{v_F^2}{\Lambda^2} y_\rho^{ik} y_\phi^{jk} = \frac{v_F^2}{\Lambda^2} \begin{pmatrix} y_\rho^{e1} & y_\rho^{\mu1} & y_\rho^{\tau1} \\ y_\rho^{e2} & y_\rho^{\mu2} & y_\rho^{\tau2} \\ y_\rho^{e3} & y_\rho^{\mu3} & y_\rho^{\tau3} \end{pmatrix} \begin{pmatrix} y_\phi^{e1} & y_\phi^{e2} & -y_\phi^{e3} \\ y_\phi^{\mu1} & y_\phi^{\mu2} & -y_\phi^{\mu3} \\ -y_\phi^{\tau1} & -y_\phi^{\tau2} & y_\phi^{\tau3} \end{pmatrix}. \quad (3.6)$$

As for the Majorana mass term $M_k \overline{N}_k^c N_k$, since the three right-handed neutrinos transform trivially under $\mathbb{D}_4 \times Z_3 \times Z_5$, we obtain a diagonal Majorana neutrino mass matrix $M_k = \text{diag}(M_1, M_2, M_3)$. Consequently, neutrino masses induced via the one-loop diagram in Fig. 2 are given by

$$\begin{aligned} (M_\nu)_{ij} &= -\frac{\mu_T \lambda_T v_\chi v_H^2 v_F^2}{m_T^2 \Lambda^2} y_\rho^{ik} M_k y_\phi^{jk} J(m_\rho^2, m_\phi^2, M_k^2) \\ &= \sum_k \frac{v_\chi}{\Lambda} y_\rho^{ik} \Gamma_k y_\phi^{jk}, \end{aligned} \quad (3.7)$$

where v_χ is the VEV of the flavon χ while Γ_k is defined as follows

$$\Gamma_k = -\frac{\mu_T v_H^2 \lambda_T M_k v_F^2}{m_T^2 \Lambda} J(m_\rho^2, m_\phi^2, M_k^2), \quad (3.8)$$

while the loop function J is defined as

$$\begin{aligned} J(m_\rho^2, m_\phi^2, M_k^2) &= -\frac{1}{(4\pi)^2} \left[\frac{m_\rho^2}{(m_\rho^2 - m_\phi^2)(m_\rho^2 - M_k^2)} \ln \frac{M_k^2}{m_\rho^2} \right. \\ &\quad \left. + \frac{m_\phi^2}{(m_\phi^2 - m_\rho^2)(m_\phi^2 - M_k^2)} \ln \frac{M_k^2}{m_\phi^2} \right]. \end{aligned} \quad (3.9)$$

Assuming for simplicity that we have a quasi-degenerate right-handed neutrino masses with $M_3 \simeq M_2 \simeq M_1$ implying $\Gamma_3 \simeq \Gamma_2 \simeq \Gamma_1$. In this case, the total neutrino mass matrix can be expressed as $M_\nu = \Gamma_1 \left[\frac{v_\chi}{\Lambda} y_\rho^{ik} y_\phi^{jk} \right]$, and by assuming the following conditions on the Yukawa couplings

$$\begin{aligned} y_\phi^{\mu 2} &= y_\phi^{\tau 2} = y_\phi^{\mu 3} = y_\phi^{\epsilon 3} = 0, \quad y_\rho^{\tau 1} = -y_\rho^{\tau 3}, \quad y_\rho^{\epsilon 1} = -y_\rho^{\epsilon 3} = -y_\rho^{\epsilon 2} \\ y_\phi^{\tau 1} &= y_\phi^{\tau 3}, \quad y_\rho^{\mu 3} = y_\rho^{\mu 2}, \quad \frac{y_\phi^{\mu 1}}{y_\rho^{\epsilon 2}} = -\frac{y_\phi^{\epsilon 1}}{y_\rho^{\mu 2}} = \frac{2y_\phi^{\epsilon 2}}{y_\rho^{\mu 1} + y_\rho^{\mu 2}}, \quad y_\rho^{\tau 2} = \frac{y_\rho^{\epsilon 2} y_\phi^{\epsilon 2}}{y_\phi^{\tau 3}}, \end{aligned} \quad (3.10)$$

we obtain the total neutrino mass matrix expressed as

$$M_\nu = \Gamma_1 \begin{pmatrix} 2a + b & -a & -b \\ -a & a & a \\ -b & a & b \end{pmatrix}, \quad (3.11)$$

where to avoid heavy notations we have introduced the following parametrization $a = \frac{v_\chi}{\Lambda} y_\rho^{\epsilon 2} y_\phi^{\epsilon 2}$ and $b = \frac{v_\chi}{\Lambda} y_\rho^{\tau 3} y_\phi^{\tau 3}$. This matrix exhibits the magic symmetry referring to the equality of the sum of each row and the sum of each column in M_ν [75]. It is well known that the mass matrix acquiring this property is diagonalized by the trimaximal mixing matrix U_{TM_2} which accounts naturally for the nonzero θ_{13} as well as a possible determination of the θ_{23} octant. Therefore, M_ν is diagonalized as $U_{TM_2}^\dagger M_\nu U_{TM_2} = \text{diag}(m_1, m_2, m_3)$ with U_{TM_2} is expressed following the PDG parametrization for the lepton mixing matrix as

$$U_{TM_2} = \begin{pmatrix} \sqrt{\frac{2}{3}} \cos \theta & \frac{1}{\sqrt{3}} & \sqrt{\frac{2}{3}} \sin \theta e^{-i\sigma} \\ -\frac{\cos \theta}{\sqrt{6}} - \frac{\sin \theta}{\sqrt{2}} e^{i\sigma} & \frac{1}{\sqrt{3}} & \frac{\cos \theta}{\sqrt{2}} - \frac{\sin \theta}{\sqrt{6}} e^{-i\sigma} \\ -\frac{\cos \theta}{\sqrt{6}} + \frac{\sin \theta}{\sqrt{2}} e^{i\sigma} & \frac{1}{\sqrt{3}} & -\frac{\cos \theta}{\sqrt{2}} - \frac{\sin \theta}{\sqrt{6}} e^{-i\sigma} \end{pmatrix} U_P \quad (3.12)$$

Here θ is an arbitrary angle that will be related to the observed neutrino mixing angles θ_{ij} , σ is an arbitrary phase that will be related later on to the Dirac CP phase δ_{CP} and $U_P = \text{diag}(1, e^{i\frac{\alpha_{21}}{2}}, e^{i\frac{\alpha_{31}}{2}})$ is a diagonal matrix that encodes the Majorana phases α_{21} and α_{31} . The Yukawa couplings in the parameters a and b are complex number of order one, hence M_ν is a complex mass matrix. To diagonalize M_ν we take b to be real without loss of generality while the parameter a remains complex; $a \rightarrow |a| e^{i\phi_a}$ where ϕ_a is a CP violating phase. As a result, we obtain the three active light neutrino masses m_1 , m_2 and m_3 expressed explicitly as

$$\begin{aligned} |m_1| &= \Gamma_1 \sqrt{|a|^2 + 4b^2 + \frac{9|a|^4}{4b^2} + |a| \left(\frac{3|a|^2}{b} + 4b \right) \cos \phi_a + 6|a|^2 \cos 2\phi_a}, \\ |m_2| &= \Gamma_1 |a|, \\ |m_3| &= \Gamma_1 \sqrt{|a|^2 + \frac{9|a|^4}{4b^2} - \frac{3|a|^3}{b} \cos \phi_a}, \end{aligned} \quad (3.13)$$

provided that $|a| < |b|$ and the following conditions on θ and σ hold

$$\tan 2\theta = -\frac{\sqrt{3(|a|^2 - b^2)^2 + 12|a|^2 b^2 \sin^2 \phi_a}}{4|a|b \cos \phi_a + 3|a|^2 + b^2}, \quad \tan \sigma = \frac{2|a|b \sin \phi_a}{|a|^2 - b^2}. \quad (3.14)$$

Regarding the mixing angles, we use the PDG standard parametrization of the Pontecorvo-Maki-Nakagawa-Sakata (PMNS) matrix [76], then we calculate the three observed neutrino mixing angles in terms of the trimaximal mixing parameters, we find

$$\begin{aligned} \sin^2 \theta_{13} &= \frac{2}{3} \sin^2 \theta, \quad \sin^2 \theta_{12} = \frac{1}{3 - 2 \sin^2 \theta} \\ \sin^2 \theta_{23} &= \frac{1}{2} - \frac{3 \sin 2\theta}{2\sqrt{3}(3 - 2 \sin^2 \theta)} \cos \sigma. \end{aligned} \quad (3.15)$$

Since the recent experimental data signals that a normal mass ordering is more preferred than an inverted ordering [77, 78], we will perform our numerical study in the normal hierarchy case. Therefore, we use as input data the results of the global analysis by NuFIT 4.0 of the neutrino oscillation parameters at 3σ interval [78] in the NH case; we have

$$\begin{aligned} \sin^2 \theta_{13} &\in [0.02044 \rightarrow 0.02437] \quad , \quad \sin^2 \theta_{23} \in [0.428 \rightarrow 0.624] \\ \sin^2 \theta_{12} &\in [0.275 \rightarrow 0.350] \quad , \quad \frac{\Delta m_{21}^2}{10^{-5}} [\text{eV}^2] \in [6.79 \rightarrow 8.01] \\ &\frac{\Delta m_{31}^2}{10^{-3}} [\text{eV}^2] \in [2.431 \rightarrow 2.622]. \end{aligned} \quad (3.16)$$

The trimaximal matrix is described by two unknown parameters θ and σ which are in turn linked to the free parameters Γ_1 , a , b and ϕ_a appearing in the neutrino mass matrix (3.11). First, by using the 3σ experimental range of $\sin^2 \theta_{13}$ and the first equation in (3.15) we find the permitted values of θ as $0.176 \lesssim \theta [\text{rad}] \lesssim 0.193$. Inserting this constraint on θ in the formula of the solar mixing angle in (3.15) allows to restrict the interval of θ_{12} compared to its 3σ allowed range (see

Eq. (3.16)) where we obtain $\sin^2 \theta_{12} \in [0.334 \rightarrow 0.341]$. Then, by using the experimental values of three mixing angles $\sin^2 \theta_{ij}$ at 3σ range, we show in the left panel of Fig. 3 the correlation between θ and the arbitrary phase σ which is randomly varied in the range $[-\pi \rightarrow \pi]$. Accordingly, we find a more constrained range for σ given by

$$\sigma [\text{rad}] \in [-3.139313 \rightarrow -0.827825] \cup [0.846743 \rightarrow 3.141149]. \quad (3.17)$$

On the other hand, since the parameters $a = \frac{v_\chi}{\Lambda} y_\rho^{e2} y_\phi^{e2}$ and $b = \frac{v_\chi}{\Lambda} y_\rho^{\tau3} y_\phi^{\tau3}$ contribute to the small

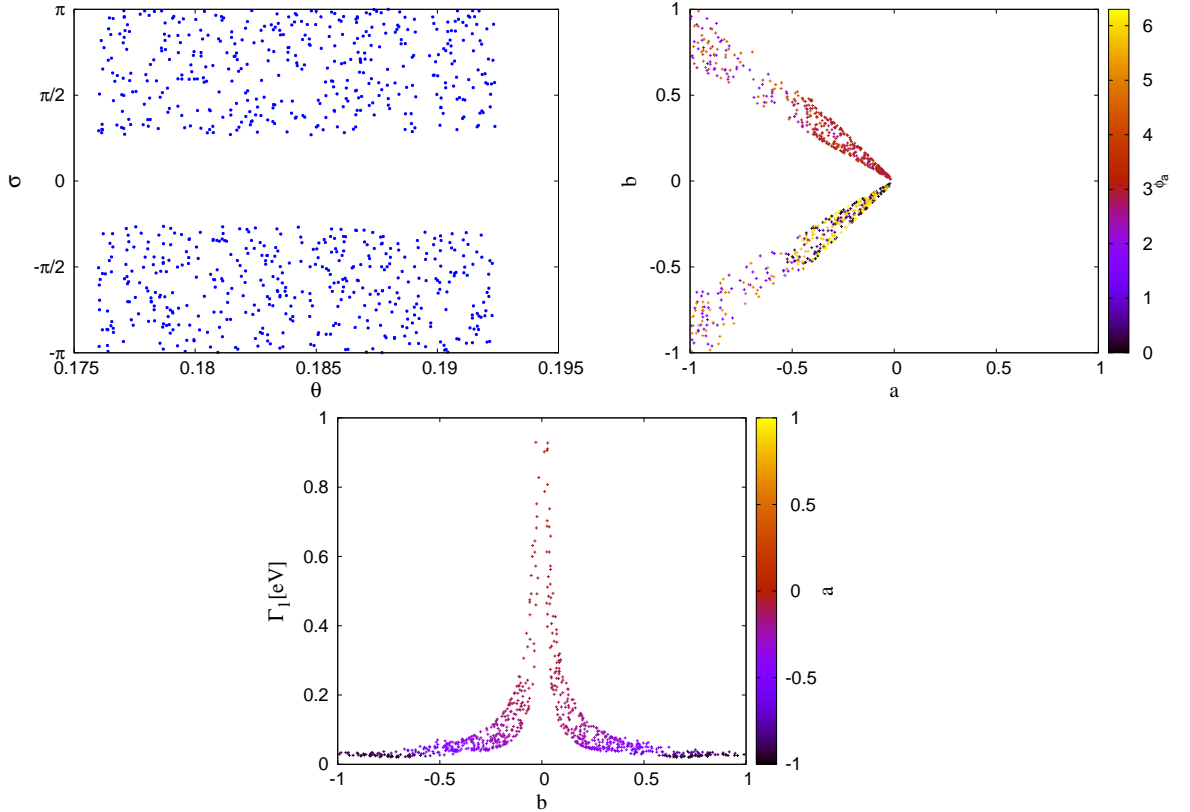


Figure 3: Left: Variation of the arbitrary phase σ as a function of the angle θ . Right: Correlation among the parameters a , b and the phase ϕ_a . Bottom: Correlation among the parameters a , b and Γ_1 .

neutrino masses, the VEV of the flavon χ needs to be small and close to the cutoff scale $v_\chi \lesssim \Lambda$ with $y_{\rho,\phi}^{e2}, y_{\rho,\phi}^{\tau3} \sim \mathcal{O}(1)$; thus, we have allowed a and b to vary in the range $-1 \lesssim a, b \lesssim 1$ while the phase ϕ_a is considered to be unrestrained; $0 \lesssim \phi_a \lesssim 2\pi$. Based on this, to get an idea about the order of magnitude of the parameter Γ_1 using Eq. (3.8), we make the obvious observation using the second equation in Eq. (3.7) that for neutrino masses around the sub-eV order, Γ_k should as well vary in the sub-eV range. However, since Γ_1 will be used as an input parameter when discussing the neutrino phenomenology, we need to fix its range. To do this, let's get an estimate

on the parameters involved on the righthand side of Eq. (3.8). Firstly, from Ref. [47] we learn that when the particles running in the loop get their masses above the EW scale and up to 1TeV , the loop function $J(m_\rho^2, m_\phi^2, M_k^2)$ gets as low as 10^{-9}GeV^{-2} . Secondly, it is well known in Type II seesaw models that the VEV of the Higgs triplet v_T is proportional to $v_T \simeq -\mu v_H^2/m_T^2$. However, in the present model the trilinear coupling μ connecting the Higgs doublets to the scalar triplet is replaced by the vertex $\lambda_T H T^\dagger H \chi$; thus, μ is equivalent to $\lambda_T v_\chi$ and eventually the quantity $-\lambda_T v_H^2/m_T^2$ in Eq. (3.8) turn out to be approximately proportional to the VEV ratio v_T/v_χ . Furthermore, the triplet VEV v_T is constrained by the experimental value of the ρ parameter $\rho_{\text{exp}} = 1.00039 \pm 0.00019$ [76], which requires $v_T \lesssim 4\text{GeV}$. At this stage, assuming that the flavons VEVs v_F and v_χ are of the same order and close to the cutoff scale and $v_T = 1\text{GeV}$, the parameter Γ_1 becomes less than or approximately equals to $\mu_T M_1 \times 10^{-9}\text{GeV}^{-1}$. Given the suppression factor $J(m_\rho^2, m_\phi^2, M_k^2) \lesssim 10^{-9}\text{GeV}^{-2}$, M_1 was assumed to lie at the TeV scale, and thus, $\Gamma_1 \lesssim 10^{-6} \times \mu_T$. Finally, the free dimension-full parameter μ_T can be chosen to be as small as 0.001GeV to get $\Gamma_1 \lesssim 1\text{eV}$. Gathering all the above information, we show in the right panel of Fig. 3 the correlation among the parameters a , b and ϕ_a while in the bottom panel of the same figure we show the correlation among Γ_1 , a and b where we used as input parameters the 3σ allowed ranges of the mass squared differences Δm_{21}^2 and Δm_{31}^2 given in (3.16). As a result, we find

$$\begin{aligned} a &\in [-0.99784 \rightarrow -0.02587] \quad , \quad b \in [-0.99955 \rightarrow 0.98998] \quad , \\ \phi_a [\text{rad}] &\in [0.00151 \rightarrow 6.28196] \quad , \quad \Gamma_1 [\text{eV}] \in [0.02044 \rightarrow 0.92926] \quad . \end{aligned} \quad (3.18)$$

3.2 Neutrino phenomenology

Given that neutrino oscillation experiments depend only on the squared-mass splittings Δm_{21}^2 and Δm_{31}^2 , there are three different approaches employed to determine the absolute scale of neutrino masses: (1) the sum of the three active neutrino masses from cosmological observations $\sum m_i \equiv m_{\text{sum}} = m_1 + m_2 + m_3$, (2) the effective neutrino mass $m_{\nu_e} = (\sum_i |U_{ei}|^2 m_i^2)^{1/2}$ using kinematic effects in beta decay experiments, and (3) the effective Majorana neutrino mass $|m_{ee}| = |\sum_i U_{ei}^2 m_i|$ in neutrinoless double beta decay ($0\nu\beta\beta$) where m_i are the three neutrino masses and U_{ei} are the elements of the first row of the mixing matrix. In our numerical study, we use the latest result from the Planck data which when combined with measurements of the baryon acoustic oscillations (BAO) provides an upper limit on m_{sum} given by $m_{\text{sum}} < 0.12\text{eV}$ at 95% C.L [79]. We start by substituting the elements of the mixing matrix and the masses defined in the above observables by their expressions given in Eqs. (3.12) and (3.13) respectively. Hence, this shows the dependence of these observables on our model parameters a , b , Γ_1 and ϕ_a as well as the parameters involved in the trimaximal mixing matrix (3.12). Then, we present our predictions using scatter plots. At first, we show in the left panel of Fig. 4 the correlations of the three neutrino masses $m_{i=1,2,3}$ and

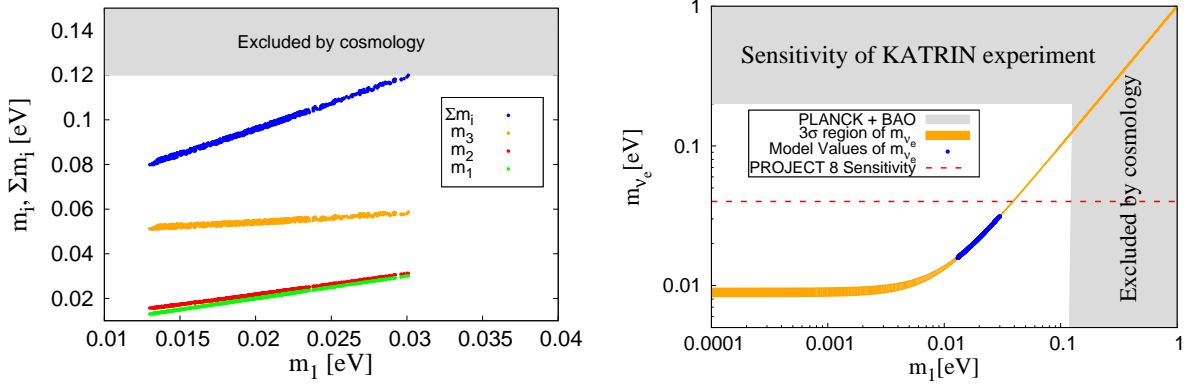


Figure 4: Left: Predictions for the absolute neutrino masses m_1 (green), m_2 (red), m_3 (orange) and their sum Σm_i (blue) as a function of the lightest neutrino mass m_1 . The horizontal gray band represent the upper limit on Σm_i provided by Planck+BAO data. Right: The effective electron neutrino mass m_{ν_e} as a function of m_1 . The vertical (horizontal) gray region is disfavored by Planck+BAO (KATRIN) data.

their sum m_{sum} versus the lightest neutrino mass m_1 where we find

$$\begin{aligned} 0.01300 &\lesssim m_1 [\text{eV}] \lesssim 0.03009 \quad , \quad 0.01561 \lesssim m_2 [\text{eV}] \lesssim 0.03124 \\ 0.05103 &\lesssim m_3 [\text{eV}] \lesssim 0.05867 \quad , \quad 0.07990 \lesssim m_{sum} [\text{eV}] \lesssim 0.11997. \end{aligned} \quad (3.19)$$

From the interval of m_1 , we take the lightest (largest) value and we replace m_2 and m_3 by $\sqrt{m_1^2 + \Delta m_{21}^2}$ and $\sqrt{m_1^2 + \Delta m_{31}^2}$ respectively, we find that the sum of neutrino masses in the normal mass hierarchy—using the best fit values of Δm_{21}^2 and Δm_{31}^2 given in [78]—requires $m_{sum} \gtrsim 0.039\text{eV}$ ($m_{sum} \gtrsim 0.09\text{eV}$). While the constraint on m_{sum} corresponding to the lightest m_1 is far from any current experiment, the upper bound on m_{sum} corresponding to the largest m_1 may be achieved in the upcoming experiments such as CORE+BAO targeting a bound on Σm_i around 0.062eV [80]. In the right panel of Fig. 4, we show the correlation between the effective mass of the electron neutrino m_{ν_e} and m_1 where the horizontal gray band indicates the expected sensitivity of m_{ν_e} from the KATRIN collaboration [81, 82]. We find that m_{ν_e} varies in the following range

$$0.01574 \lesssim m_{\nu_e} [\text{eV}] \lesssim 0.03133. \quad (3.20)$$

Clearly, the values in this interval are very small when compared with the forthcoming β -decay experiment sensitivities such as KATRIN [81, 82], HOLMES [83], and Project 8 [84] which will investigate m_{ν_e} at 0.2eV, 0.1eV and 0.04eV respectively. If none of these experiments would measure m_{ν_e} , our predicted values could be probed by future experiments aiming to reach improved sensitivities around 0.01eV. Now, let us explore the effective Majorana neutrino mass parameter of neutrinoless double beta decay $|m_{ee}|$. A positive signal of $0\nu\beta\beta$ would assert the Majorana nature

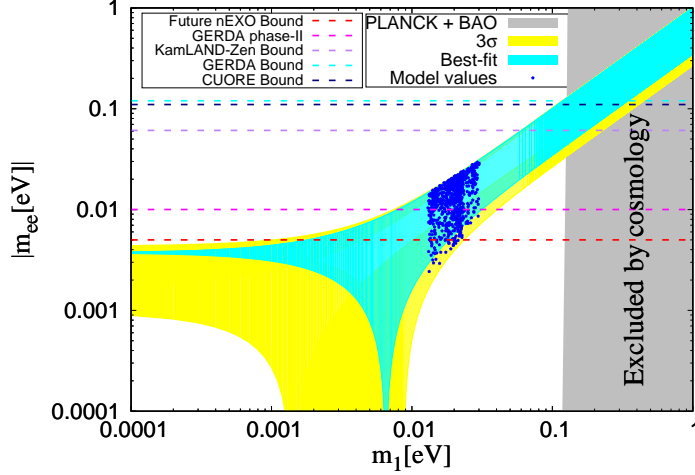


Figure 5: The effective Majorana mass $|m_{ee}|$ as a function of the lightest neutrino mass m_1 . The vertical gray region indicates the upper limit on the sum of the three light neutrino masses from Planck+BAO data.

of neutrinos as well as provide a measure of the absolute neutrino mass scale. There are many ongoing and upcoming experiments around the world setting as their purpose the detection of this process, where the present bounds on $|m_{ee}|$ come from the KamLAND-Zen [85], CUORE [86] and GERDA [87] experiments corresponding to $|m_{ee}| < (0.061 - 0.165) \text{ eV}$, $|m_{ee}| < (0.11 - 0.5) \text{ eV}$ and $|m_{ee}| < (0.15 - 0.33) \text{ eV}$ respectively. In Fig. 5, we show the correlation between $|m_{ee}|$ and the lightest neutrino mass m_1 where we use the known 3σ ranges of the oscillation parameters while we allow all phases to vary between 0 and 2π . Thus, the interval of $|m_{ee}|$ is given by

$$0.00316 \lesssim |m_{ee}| [\text{eV}] \lesssim 0.02949. \quad (3.21)$$

As a result, our predicted region is far from the current sensitivities as can be seen from the horizontal dashed lines in Fig. 5 displaying the bounds on $|m_{ee}|$ from some of the ongoing $0\nu\beta\beta$ decay experiments. On the other hand, the anticipated sensitivities of the next-generation experiments such as GERDA Phase II ($|m_{ee}| \sim (0.01 - 0.02) \text{ eV}$) [88] and nEXO ($|m_{ee}| \sim 0.005 \text{ eV}$) [89] will cover our model predictions on $|m_{ee}|$.

On a different note, the expression for Jarlskog rephasing quantity $J_{CP} = \text{Im}(U_{e1}U_{\mu 1}^*U_{\mu 2}U_{e2}^*)$ which is a measure of CP violation, is given in terms of the trimaximal parameters σ and θ as follows

$$J_{CP} = \frac{\sin 2\theta \sin \sigma}{6\sqrt{3}}. \quad (3.22)$$

On the other hand, by matching the expressions of the rephasing invariant J_{CP} in the standard parametrization of the PMNS matrix and in the trimaximal matrix defined in Eq. (3.12), we derive the relation between the Dirac CP phase δ_{CP} and the arbitrary phase σ given as $\sin \sigma =$

$\sin 2\theta_{23} \sin \delta_{CP}$. Moreover, recall that the trimaximal mixing approach used in this model restricts the atmospheric angle θ_{23} around its maximal value (but not exactly maximal $\theta_{23} \neq 45$) while the δ_{CP} phase falls in the close vicinity of $\delta_{CP} \simeq 0.5\pi$ and $\delta_{CP} \simeq -0.5\pi$. In this regards, we

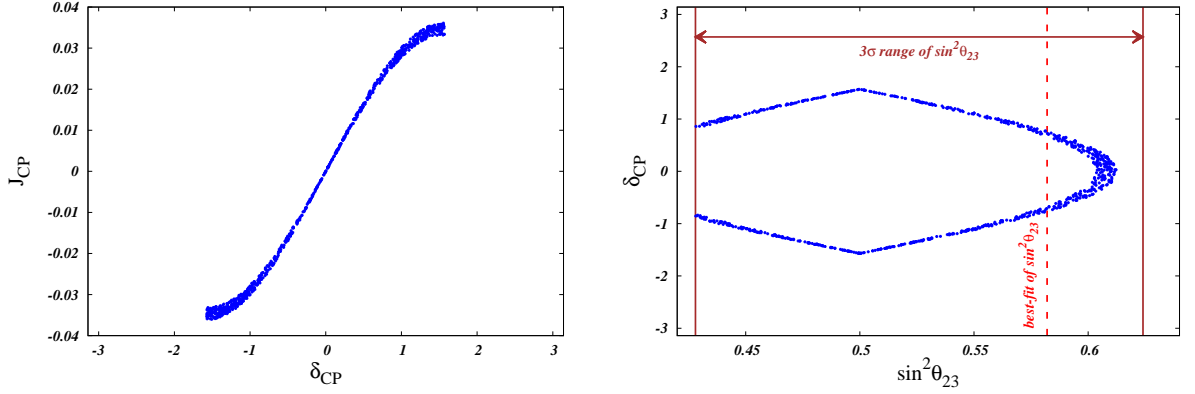


Figure 6: Left : Correlation between the Jarlskog invariant J_{CP} and the CP-violating phase δ_{CP} . Right: Correlation between δ_{CP} and the atmospheric angle $\sin^2 \theta_{23}$.

show in left panel of Fig. 6 the correlation between J_{CP} and the δ_{CP} phase where we used the equation relating δ_{CP} with σ as an input, and since we have the same parameter scan as before, the obtained range for the arbitrary phase σ is as in Eq. (3.17) while for δ_{CP} we find

$$-0.499\pi \lesssim \delta_{CP} [\text{rad}] \lesssim 0.498\pi. \quad (3.23)$$

Based on Eq. (3.22) and the obtained ranges of θ and σ ; it is straightforward to verify that $\sin 2\theta \neq 0$ and $\sin \sigma \neq 0$, subsequently leading to a non vanishing $J_{CP} \neq 0$. On the other hand, it is clear from Eq. (3.15) that the maximal value of the atmospheric angle ($\sin^2 \theta_{23} = 1/2$) is excluded in our model. Moreover, since the CP phase is correlated significantly with $\sin^2 \theta_{23}$ than the other mixing angles, we show in the right panel of Fig. 6 the predicted regions of δ_{CP} versus $\sin^2 \theta_{23}$ at 3σ . As can be seen, our model allows $\sin^2 \theta_{23}$ to vary randomly in the interval $[0.428 \rightarrow 0.612]$ where the corresponding region of δ_{CP} is as in Eq. (3.23).

4 Dark Matter candidates

Before we provide the possible DM candidates in the present model, let us discuss the breaking pattern of the G_f flavor group. First, recall that our model involves three scalar fields that acquire VEVs; the usual $SU(2)_L$ Higgs doublet H and two flavon fields F and χ . The Higgs doublet H transforms trivially under G_f and thus, it only contributes to the EW symmetry breaking. On the other hand, the flavons F and χ transform respectively as a doublet and a trivial singlet under

\mathbb{D}_4 . Therefore, only the nontrivial VEV of F is responsible for breaking the \mathbb{D}_4 symmetry down to one of its subgroups³ $G_r \subset \mathbb{D}_4$. Moreover, since these three scalar fields are chosen to be even under the additional Z_2 symmetry, this latter remains unbroken. To determine the remnant G_r symmetry that survives the \mathbb{D}_4 breaking, we recall that \mathbb{D}_4 is isomorphic to the semidirect product $Z_4 \rtimes Z'_2$ and has two generators S and T where S generates Z_4 and T generates Z'_2 symmetries satisfying the relations $S^4 = T^2 = Id$ and $STS = T$. Recall also that the VEV alignment of the flavon F — $\langle F \rangle = v_F(1, 1)$ —is chosen to reproduce the observed neutrino masses and mixing. This specific VEV direction breaks \mathbb{D}_4 down to Z'_2 with broken part given by the Z_4 group. This means that the VEV structure of the flavon F preserves the generator T while changes the generator S ; we have⁴

$$T \langle F \rangle = \langle F \rangle \quad , \quad S \langle F \rangle \neq \langle F \rangle . \quad (4.1)$$

Therefore, the spontaneous breaking of the full discrete flavor symmetry G_f is given by

$$\mathbb{D}_4 \times Z_3 \times Z_5 \times Z_2 \xrightarrow{\langle F \rangle, \langle \chi \rangle} Z'_2 \times Z_2 . \quad (4.2)$$

Now, we are in position to discuss the stabilization of the DM candidates by the remnant $Z'_2 \times Z_2$ symmetry. For this purpose, let us first briefly comment these reflection symmetries individually. On the one hand, for the residual Z'_2 symmetry, it is useful to study the decomposition of \mathbb{D}_4 irreducible representations into those of its subgroup Z'_2 . The latter has two singlet representations 1_+ (trivial) and 1_- , and from the characters of the \mathbb{D}_4 group (see Table 4 in the Appendix), it is easy to check that the singlet representations $1_{+,+}$ and $1_{+,-}$ of \mathbb{D}_4 correspond to 1_+ of Z'_2 , while $1_{-,+}$ and 1_{--} of \mathbb{D}_4 correspond to 1_- of Z'_2 . For the \mathbb{D}_4 doublet 2 , it decomposes into Z'_2 representations as $2 = 1_+ + 1_-$ where the first component of 2 is associated to 1_+ while the second one is associated to 1_- . Therefore, the particles running in the loop transform under the Z'_2 symmetry as

$$\begin{aligned} N_1 &\rightarrow N_1 \quad , \quad N_2 \rightarrow N_2 \quad , \quad N_3 \rightarrow -N_3 \\ \rho &\rightarrow \rho \quad , \quad \phi \rightarrow \phi \end{aligned} \quad (4.3)$$

From these transformations, it is easy to notice that this remaining Z'_2 symmetry is not sufficient for DM stabilization. For example, in the case where ρ is the DM candidate, the couplings $\bar{L}_i l_i^R \rho$ with $i = e, \mu, \tau$ are protected by Z'_2 after symmetry breaking, therefore these couplings lead to the DM decay $\rho \rightarrow \bar{L}_i l_i^R$.

On the other hand, the particles in (4.3) are odd under the extra symmetry Z_2 whilst all SM particles are even under it. This clearly shows that this extra symmetry stabilizes these potential DM particles against decay into SM ones. Therefore, the DM candidate in our model is the lightest among the fermionic right-handed neutrinos N_k and the scalars ρ and ϕ . Moreover, since the full residual flavor symmetry in the neutrino sector is $Z'_2 \times Z_2$ group, there might be processes

³Notice that since the flavon field χ carries the charges ω and η^4 under Z_3 and Z_5 respectively, these groups are spontaneously broken to the identity.

⁴See the matrix representation of the \mathbb{D}_4 generators in the Appendix.

allowed by Z_2 but forbidden by Z'_2 . Thus, it is important to verify the invariance of the various DM processes under Z_2 as well as Z'_2 . Here, we will discuss briefly the possible DM candidates while a thorough calculation of their properties such as annihilation cross section, lifetime and relic abundance is beyond the purpose of the present work.

As mentioned above, all the particles running in the loop diagram of Fig. 2 are potential DM candidates. In the following, we discuss two possibilities:

Case I: Fermionic dark matter candidate

In order to facilitate the engineering of neutrino masses and mixing, we have considered the case where $M_3 \simeq M_2 \simeq M_1$. We assume here for simplicity that N_3 is the only fermionic DM candidate. In this scenario, a pair of N_3 can annihilate into SM particle pair $N_3 N_3 \rightarrow l^+ l^- (\nu \bar{\nu})$ through t-channel diagrams mediated by the components of scalar doublets ρ and ϕ given in (3.4). Moreover, it is well known that the dark matter abundance depends not only on the annihilation cross section, but for quasi-degenerate states the co-annihilation cross section becomes important. In the present case, since the neutrino masses M_1 and M_2 are close to M_3 (which implies the relative mass difference $\Delta_i = \frac{(M_i - M_3)}{M_3} \ll 1$), then the co-annihilation processes of $N_3 N_1$ and $N_3 N_2$ into charged leptons $l^+ l^-$ and neutrino $\nu \bar{\nu}$ dominate over the annihilation processes. On the other hand, since the right handed neutrino N_3 transforms as an $SU(2)_L$ singlet, it has no tree level couplings to the Higgs boson or the Z boson. However, due to the Majorana nature of the DM particle, the spin independent (SI) scattering cross section of N_3 on nucleons takes place via the effective coupling $y_{hN_3 N_3}$ that induces the one-loop effective coupling between DM and the Higgs boson [90,91].

The right handed neutrino as a suitable DM candidate have been studied in several radiative neutrino models with inert Higgs doublet, see for example [42,92]. In particular, as a result of the analysis performed in reference⁵ [42], the RH neutrino is a promising DM candidate in the mass range $10 < m_{DM} \text{ (GeV)} < 700$. This region is in agreement with the relic abundance measured by WMAP [93] and Planck [94] collaborations and with a SI direct detection cross section below the upper limits given by Lux [95] and Xenon1T [96] experiments.

Case II: Scalar dark matter candidate

We assume that the DM candidate is one of the neutral components of the inert scalar doublet ρ (ρ_1 or ρ_2) and it is lighter than the flavon fields χ and F and the members of the scalar triplet T . Therefore, the relic abundance of DM can only be determined by its annihilation/co-annihilation to SM particles. Moreover, since ρ is an EW doublet, it is well known that such processes are mediated by SM Higgs and gauge bosons. The relevant invariant terms involving the inert doublet

⁵The involved processes for annihilation, co-annihilation as well as SI scattering of DM in this study are roughly similar to the ones involved in our model.

ρ in the scalar potential can be written as

$$\begin{aligned} \mathcal{V}(\rho) \supset & \mu_\rho^2 |\rho|^2 + 2\lambda_1 (\rho^\dagger \rho)^2 + 2\lambda_2 (\rho^\dagger F_1)(\rho F_1^\dagger) + 2\lambda_3 (\rho^\dagger \rho)(F F^\dagger) \\ & + \lambda_4 (H^\dagger H)(\rho^\dagger \rho) + \lambda_5 (H^\dagger \rho)(\rho^\dagger H) + \lambda_6 (\rho^\dagger \chi)(\rho \chi^\dagger) + \lambda_7 (\rho^\dagger \rho)(\chi^\dagger \chi) \\ & + \lambda_8 (\rho^\dagger \rho) Tr(T^\dagger T) + \lambda_9 \rho^\dagger T T^\dagger \rho \end{aligned} \quad (4.4)$$

As mentioned above, the SM Higgs doublet H , the triplet Higgs T and the flavon singlets F and χ can develop VEVs while the inert doublet ρ does not develop a VEV. This can be parameterized as

$$\begin{aligned} \langle H \rangle &= \frac{1}{\sqrt{2}} \begin{pmatrix} 0 \\ v_H + h \end{pmatrix}, \quad \rho = \frac{1}{\sqrt{2}} \begin{pmatrix} \rho_1 + i\rho_2 \\ \sqrt{2}\rho^- \end{pmatrix} \\ \langle T \rangle &= \frac{1}{\sqrt{2}} \begin{pmatrix} 0 & 0 \\ v_T + T & 0 \end{pmatrix}, \quad \langle F \rangle = \frac{1}{\sqrt{2}} (v_F + F), \quad \langle \chi \rangle = \frac{1}{\sqrt{2}} (v_\chi + \chi) \end{aligned} \quad (4.5)$$

where we have omitted the pseudo scalars for all the fields except for ρ . From this parametrization, we find the masses of the physical states ρ_1 , ρ_2 and ρ^\pm in terms of parameters of the potential $\mathcal{V}(\rho)$ as

$$\begin{aligned} M_{\rho_1, \rho_2}^2 &= \mu_\rho^2 + (\lambda_2 + \lambda_3) v_F^2 + \frac{\lambda_4}{2} v_H^2 + \frac{1}{2} (\lambda_6 + \lambda_7) v_\chi^2 + \frac{\lambda_8}{2} v_T^2 \\ M_{\rho^\pm}^2 &= \mu_\rho^2 + (\lambda_2 + \lambda_3) v_F^2 + \frac{1}{2} (\lambda_4 + \lambda_5) v_H^2 + \frac{1}{2} (\lambda_6 + \lambda_7) v_\chi^2 + \frac{1}{2} (\lambda_8 + \lambda_9) v_T^2 \end{aligned} \quad (4.6)$$

As a result, we obtain a mass degeneracy between ρ_1 and ρ_2 and thus we cannot distinguish between them in the present model. This degeneracy is due to the vanishing of the coupling $\{\lambda_\rho (H\rho)^2 + h.c.\}$ which is—as in the usual inert doublet model (IDM) [97]—responsible for the mass splitting of the neutral components ρ_1 and ρ_2 of the inert doublet ρ after EW symmetry breaking. The λ_ρ term is actually invariant under all the symmetries of the model; however, due to the \mathbb{D}_4 structure of ρ given in (3.5) the tensor product⁶ $\hat{\rho} \otimes \hat{\rho}|_{1_{++}}$ vanishes according to Eq. (6.2) in the appendix. Therefore, the \mathbb{D}_4 structure of ρ preserves the mass degeneracy between ρ_1 and ρ_2 . Reasoning from this outcome and the fact that the couplings of DM particles with gauge bosons relate directly to the cross section for scattering off a nucleus, the DM-quark inelastic scattering $\rho_1 q \rightarrow \rho_2 q$ can be described by the unsuppressed vertex coupling $Z - \rho_1 - \rho_2$ whose size is fixed by the EW gauge coupling. Such DM inelastic scattering scenario predicts a large cross section in the direct detection experiments and has already excluded by the current results [98–100].

Regardless of the smallness of the mass splitting required to fit the experimental data, one way to allow a mass splitting between the neutral component of the inert scalar ρ in the present model is by modifying the \mathbb{D}_4 irreducible representation of ρ where if it is assigned to one of the \mathbb{D}_4 singlets instead of the \mathbb{D}_4 doublet, the λ_ρ term will be allowed and then, the mass splitting between ρ_1 and

⁶The hat in $\hat{\rho}$ denotes a \mathbb{D}_4 doublet while ρ without the hat character denotes the $SU(2)_L$ inert doublet; see Eq. (3.5).

ρ_2 will depend on the size of this quartic coupling λ_ρ . However, assigning the \mathbb{D}_4 doublet to ρ is required to make the topology T4-2-i genuine which is our primary concern in the present study. Notice by the way that the discussion on ρ holds as well for the case of the scalar ϕ where by replacing ρ by ϕ in Eq. (4.4), we end up with the same conclusion for the masses of the chargeless components of ϕ .

5 Conclusion

In this work, we have proposed a radiative neutrino model based on topology T4-2-i providing an explanation for the observed neutrino masses and mixing as well as allowing for stable dark matter candidates. In order to avoid the tree level Type I and Type II seesaw contributions always accompanying topology T4-2-i, fitting the neutrino data as well as to ensure the stability of DM candidates, we have extended the SM gauge symmetry with the $G_f = \mathbb{D}_4 \times Z_3 \times Z_5 \times Z_2$ flavor group. For this purpose, besides promoting the fermion in topology T4-2-i to singlet right-handed neutrinos N_k , we have added two flavon fields F and χ to guarantee the invariance of neutrino Yukawa couplings and the preexisting vertex $\mu_H HT^\dagger H$ connecting two Higgs doublets with the scalar triplet T . Therefore, the neutrino masses are radiatively generated at one-loop level while their mixing is described by the well known TM_2 pattern due to G_f symmetry breaking.

We have performed our numerical study in the normal mass hierarchy case where we have shown through several scatter plots the allowed ranges of our model parameters $\{\sigma, \theta, a, b, \phi_a, \Gamma_1\}$, which we have used to predict the ranges of the CP violating phase δ_{CP} as well as the non-oscillatory observables m_{ν_e} , $|m_{ee}|$ and m_{sum} that fit the experimental values of the three mixing angles θ_{ij} and the mass square differences Δm_{ij}^2 at 3σ range.

Another matter considered in the present work is the dark matter candidates given by one of the fields running in the loop. On the basis of our considerations, the DM candidates can be manifested by the neutral components of the scalar doublets ρ and ϕ , and the right-handed neutrino N_3 , the lightest of which can play the role of DM as they carry odd charge under Z_2 . We showed that the stability of DM is guaranteed by the unbroken Z_2 symmetry while the different DM processes are controlled by the residual group $Z'_2 \times Z_2$ after G_f symmetry breaking. In the case of the inert scalar ρ , we found that there are no mass splitting between its neutral components where in the scenario of DM inelastic scattering predicts a large cross section in the direct detection experiments and has already excluded by the current data. On the other hand, in the case of Majorana DM, N_3 is a suitable candidate because the relevant processes for annihilation, co-annihilation as well as SI scattering of DM in our study are roughly similar to the ones involved in radiative models with right-handed Majorana DM. We should mention however that a thorough study of the latter case requires performing further studies by analysing two particular experimental constraints; the observed DM relic density and the cross section for direct detection of DM scattering off nucleon. This analysis, however, goes beyond the scope of this paper.

6 Appendix: Dihedral \mathbb{D}_4 group

In this appendix, we briefly review the basic features of the dihedral group \mathbb{D}_4 as well as the decomposition of its representations into those of the Z'_2 subgroup. Recall first that the discrete group \mathbb{D}_4 is generated by the two elements S and T which fulfill the relations $S^4 = T^2 = Id$ and $STS = T$. It has five irreducible representations; four singlets $1_{+,+}, 1_{+,-}, 1_{-,+}$ and $1_{-,-}$, and one doublets 2 where the indices in the representations refer to their characters under S and T as in the following table. The generators S and T of the two-dimensional representations can be expressed

$\chi_{i,j}$	$\chi_{1_{+,+}}$	$\chi_{1_{+,-}}$	$\chi_{1_{-,+}}$	$\chi_{1_{-,-}}$	$\chi_{2_{0,0}}$
Id	+1	+1	+1	+1	2
S	+1	-1	+1	-1	0
T	+1	+1	-1	-1	0

Table 4: Character table of the dihedral group \mathbb{D}_4 .

by the following 2×2 matrices

$$S = \begin{pmatrix} i & 0 \\ 0 & -i \end{pmatrix}, \quad T = \begin{pmatrix} 0 & 1 \\ 1 & 0 \end{pmatrix}. \quad (6.1)$$

Now, we consider tensor products of \mathbb{D}_4 irreducible representations. The tensor product of two doublets $2_x = (x_1, x_2)^T$ and $2_y = (y_1, y_2)^T$ is decomposed into a sum of \mathbb{D}_4 singlet representations as $2_x \times 2_y = 1_{+,+} + 1_{+,-} + 1_{-,+} + 1_{-,-}$, where

$$\begin{aligned} 1_{+,+} &= x_1 y_2 + x_2 y_1, & 1_{+,-} &= x_1 y_1 + x_2 y_2 \\ 1_{-,+} &= x_1 y_2 - x_2 y_1, & 1_{-,-} &= x_1 y_1 - x_2 y_2 \end{aligned} \quad (6.2)$$

whereas the product between two singlets is as follows

$$1_{i,j} \times 1_{k,l} = 1_{ik,jl} \quad \text{with } i, j, k, l = \pm. \quad (6.3)$$

Finally, since the experimental data on neutrino masses and mixing angles require the breaking of \mathbb{D}_4 down to its remnant Z'_2 subgroup, so we restrict our discussion only to the breaking pattern $\mathbb{D}_4 \xrightarrow{\langle F \rangle} Z'_2$. After this stage of breaking, it is obvious that the matter and scalar fields in our model will be charged under the unbroken discrete symmetry Z'_2 . Accordingly, we summarize in the following table the decompositions of \mathbb{D}_4 irreducible representations into those of the residual group Z'_2 subgroup

Fields under \mathbb{D}_4 Irreps.		Decomposition into Z'_2 Irreps.
$\begin{pmatrix} \alpha_1 \\ \alpha_2 \end{pmatrix} \sim 2$	\rightarrow	$\alpha_1 \sim +1$ $\alpha_2 \sim -1$
$\beta_1 \sim 1_{+,+}, \beta_2 \sim 1_{+,-}$	\rightarrow	$\beta_1, \beta_2 \sim +1$
$\gamma_1 \sim 1_{-,+}, \gamma_2 \sim 1_{-,-}$	\rightarrow	$\gamma_1, \gamma_2 \sim -1$

where α_i , β_i and γ_i can be any fermionic or bosonic field. For more details on the \mathbb{D}_4 Dihedral group see for instance Ref. [101].

References

- [1] T. Kajita, Rev. Mod. Phys. **88**, 030501 (2016).
- [2] A. B. McDonald, Rev. Mod. Phys. **88**, 030502 (2016).
- [3] G. Bertone, D. Hooper, and J. Silk, Phys. Rept. **405** (2005) 279–390.
- [4] S. Jana, P. K. Vishnu and S. Saad, arXiv:1910.09537 [hep-ph].
- [5] E. Ma, Phys. Rev. D **73**, 077301 (2006).
- [6] T. Hambye, K. Kannike, E. Ma, and M. Raidal, Phys. Rev. D **75**, 095003 (2007).
- [7] E. Ma and D. Suematsu, Mod. Phys. Lett. A **24** 583–589 (2009).
- [8] Y. Farzan, Phys. Rev. D **80**, 073009 (2009).
- [9] P. Fileviez Perez and M. B. Wise, Phys. Rev. D **80**, 053006 (2009).
- [10] D. Suematsu, T. Toma, and T. Yoshida, Phys. Rev. D **79**, 093004 (2009).
- [11] Y. Farzan, S. Pascoli and M. A. Schmidt, J. High Energy Phys. 10 (2010) 111.
- [12] D. Suematsu, T. Toma, and T. Yoshida, Phys. Rev. D **82**, 013012 (2010).
- [13] Y. Cai, X.-G. He, M. Ramsey-Musolf, and L.-H. Tsai, J. High Energy Phys. 12 (2011) 054.
- [14] S. Kanemura, O. Seto, and T. Shimomura, Phys. Rev. D **84**, 016004 (2011).
- [15] C.-H. Chen and S. S. C. Law, Phys. Rev. D **85**, 055012 (2012).
- [16] D. Schmidt, T. Schwetz, and T. Toma, Phys. Rev. D **85**, 073009 (2012).
- [17] M. Aoki, M. Duerr, J. Kubo, and H. Takano, Phys. Rev. D **86**, 076015 (2012).
- [18] D. Hehn and A. Ibarra, Phys. Lett. B **718**, 988 (2012).
- [19] P. S. B. Dev and A. Pilaftsis, Phys. Rev. D **86**, 113001 (2012).
- [20] S. S. C. Law and K. L. McDonald, J. High Energy Phys. 09 (2013) 092.
- [21] E. Ma, I. Picek, and Branimir Radovčić, Phys. Lett. B **726**, 744–746 (2013).

- [22] M. Hirsch, R. A. Lineros, S. Morisi, J. Palacio, N. Rojas, and J. M. F. Valle, J. High Energy Phys. 10, 149 (2013).
- [23] D. Restrepo, O. Zapata, and C. E. Yaguna, J. High Energy Phys. 11 (2013) 011.
- [24] V. Brdar, I. Picek, and B. Radovčić, Phys. Lett. B **728**, 198 (2014).
- [25] T. Toma and A. Vicente, J. High Energy Phys. 01, 160 (2014).
- [26] T. A. Chowdhury and S. Nasri, J. High Energy Phys. 12 (2015) 040.
- [27] A. Vicente and C. E. Yaguna, J. High Energy Phys. 02, 144 (2015).
- [28] W. Chao, Int. J. Mod. Phys. A **30**, 1550007 (2015).
- [29] F. von der Pahlen, G. Palacio, D. Restrepo and O. Zapata, Phys. Rev. D **94**, 033005 (2016).
- [30] S. Fraser, C. Kownacki, E. Ma, and O. Popov, Phys. Rev. D **93**, 013021 (2016).
- [31] R. Adhikari, D. Borah, and E. Ma, Phys. Lett. B **755**, 414 (2016).
- [32] E. Ma, Phys. Lett. B **755**, 348 (2016).
- [33] A. Arhrib, C. Boehm, E. Ma, and T. C. Yuan, J. Cosmol. Astropart. Phys. 04, 049 (2016).
- [34] A. Ahriche, K. L. McDonald, S. Nasri, and I. Picek, Phys. Lett. B **757**, 399 (2016).
- [35] W. B. Lu, and P. H. Gu, J. Cosmol. Astropart. Phys. 05, 040 (2016).
- [36] Y. Cai and M. A. Schmidt, J. High Energy Phys. 05, 028 (2016).
- [37] A. Ibarra, C. E. Yaguna, and O. Zapata, Phys. Rev. D **93**, 035012 (2016).
- [38] M. Lindner, M. Platscher, C. E. Yaguna, and A. Merle, Phys. Rev. D **94**, 115027 (2016).
- [39] A. Das, T. Nomura, H. Okada, and S. Roy, Phys. Rev. D **96**, 075001 (2017).
- [40] S. Singirala, Chin. Phys. C **41**, 043102 (2017).
- [41] T. Kitabayashi, S. Ohkawa, and M. Yasuè, Int. J. Mod. Phys. A **32**, 1750186 (2017).
- [42] A. Ahriche, A. Jueid, and S. Nasri, Phys. Rev. D **97**, 095012 (2018).
- [43] T. Nomura and H. Okada, Phys. Dark Univ. 21, 90-95 (2018).
- [44] N. Rojas, R. Srivastava, and J. W. F. Valle, Phys. Lett. B **789**, 132 (2019).
- [45] T. Kitabayashi, Phys. Rev. D **98**, 083011 (2018).

- [46] A. Ahriche, A. Arhrib, A. Jueid, S. Nasri, and A. de la Puente, Phys. Rev. D **101**, 035038 (2020).
- [47] F. Bonnet, M. Hirsch, T. Ota, and W. Winter, J. High Energy Phys. 07, 153 (2012).
- [48] D. Aristizabal Sierra, A. Degee, L. Dorame, and M. Hirsch, J. High Energy Phys. 03, 040 (2015).
- [49] Q. H. Cao, S. L. Chen, E. Ma, B. Yan and D. M. Zhang, Phys. Lett. B **779**, 430 (2018).
- [50] R. Cepedello, R. M. Fonseca and M. Hirsch, J. High Energy Phys. 06, 34 (2018)/J. High Energy Phys. 10, 197 (2018).
- [51] Y. Cai, J. Herrero-Garcia, M. A. Schmidt, A. Vicente, and R. R. Volkas, Front.in Phys. **5**, 63 (2017).
- [52] E. Ma, Phys. Lett. B **671**, 366 (2009).
- [53] E. Ma, A. Natale and A. Rashed, Int. J. Mod. Phys. A **27**, (2012) 1250134.
- [54] E. Ma, Phys. Rev. D **87**, 097301 (2013).
- [55] A. E. Carcamo Hernandez, I. de Medeiros Varzielas, S. G. Kovalenko, H. Päs and I. Schmidt, Phys. Rev. D **88**, 076014 (2013).
- [56] M. D. Campos, A. E. Cárcamo Hernández, S. Kovalenko, I. Schmidt and E. Schumacher, Phys. Rev. D **90**, 016006 (2014).
- [57] A. Adulpravitchai, M. Lindner and A. Merle, Phys. Rev. D **80**, 055031 (2009).
- [58] E. Ma, Phys. Lett. B **723**, 161 (2013).
- [59] E. Ma and A. Natale, Phys. Lett. B **734**, 403–405 (2014).
- [60] E. C. F. S. Fortes, A. C. B. Machado and J. Montaña and V. Pleitez, Phys. Lett. B **803**, 135289 (2020).
- [61] S. Pramanick, Phys. Rev. D **100**, 035009 (2019).
- [62] D. Meloni, S. Morisi and E. Peinado, Phys. Lett. B **703**, 281-287 (2011).
- [63] A. Biswas and A. Shaw, JCAP **1802**, 029 (2018).
- [64] A. Dasgupta and D. Borah, Nucl. Phys. **B889**, 637 (2014).
- [65] N. Haba, A. Watanabe and K. Yoshioka, Phys. Rev. Lett. **97** (2006) 041601.
- [66] X. G. He and A. Zee, Phys. Lett. B **645**, (2007) 427.

- [67] W. Grimus and L. Lavoura, J. High Energy Phys. 0809, 106 (2008).
- [68] H. Ishimori, Y. Shimizu, M. Tanimoto and A. Watanabe, Phys. Rev. D **83**, 033004 (2011).
- [69] Y. Shimizu, M. Tanimoto, A. Watanabe, Prog. Theor. Phys. **126** (2011) 81-90.
- [70] X. G. He, A. Zee, Phys. Rev. D **84**, 053004 (2011).
- [71] I. de M. Varzielas and D. Pidt, J. High Energy Phys. 03, 065 (2013).
- [72] Y. Cai, J. D. Clarke, M. A. Schmidt, and R. R. Volkas, J. High Energy Phys. 02, 161 (2015).
- [73] R. Cepedello, M. Hirsch, and J. C. Helo, J. High Energy Phys. 07, 079 (2017).
- [74] C. D. Froggatt and H. B. Nielsen, Nucl. Phys. **B147**, 277 (1979).
- [75] C. S. Lam, Phys. Rev. D **74**, 113004 (2006).
- [76] M. Tanabashi et al. (Particle Data Group), Phys. Rev. D **98**, 030001 (2018).
- [77] P. F. de Salas, S. Gariazzo, O. Mena, C. A. Ternes, and M. Tórtola, Front. Astron. Space Sci. 5 (2018) 36.
- [78] I. Esteban, M. C. Gonzalez-Garcia, A. Hernandez-Cabezudo, M. Maltoni and T. Schwetz, J. High Energy Phys. 01, 106 (2019).
- [79] Planck Collaboration and N. Aghanim et al., arXiv:1807.06209 (2018).
- [80] CORE Collaboration, E. Di Valentino et al., J. Cosmol. Astropart. Phys. 1804, 017 (2018).
- [81] KATRIN, J. Angrik et al., “KATRIN design report 2004,”.
- [82] S. Mertens, Phys. Procedia 61, 267 (2015).
- [83] A. Nucciottiet al., J. Low. Temp. Phys. 193 (2018), no. 5-6 1137–1145.
- [84] Project 8 Collaboration, A. A. Esfahani et al., J. Phys. G **44** (2017) 054004.
- [85] A. Gando et al. (KamLAND-Zen Collaboration), Phys. Rev. Lett. **117**, 082503 (2016).
- [86] C. Alduino et al. (CUORE Collaboration), Phys. Rev. Lett. **120**, 132501 (2018).
- [87] M. Agostini et al. (GERDA Collaboration), Phys. Rev. Lett. **111**, 122503 (2013).
- [88] M. Agostini et al. (GERDA Collaboration), Nature **544** (2017) 47–52.
- [89] J. B. Albert et al. (nEXO Collaboration), Phys. Rev. C **97**, 065503 (2018).
- [90] U. Haisch and F. Kahlhoefer, JCAP 1304 (2013) 050.

- [91] J. H. Garcia, E. Molinaro and M. A. Schmidt, Eur. Phys. J. C 78 (2018) 6, 471.
- [92] A. Ahriche, K. L. Mc Donald and S. Nasri, JHEP 1606,182 (2016).
- [93] G.Hinshaw et al. [WMAP Collaboration], Astrophys. J. Suppl. 208, 19 (2013)
- [94] P. A. R. Ade et al. [Planck Collaboration], Astron. Astrophys. 594, A13(2016).
- [95] D. S. Akerib et al. [LUX Collaboration], Phys. Rev. Lett. 118 (2017) no.2, 021303.
- [96] E. Aprile et al. [XENON Collaboration], Phys. Rev. Lett. 119,no.18, 181301 (2017).
- [97] N. G. Deshpande and E. Ma, Phys. Rev. D 18 (1978) 2574.
- [98] C. Arina, F.-S. Ling and M. H. Tytgat, JCAP 10 (2009) 018.
- [99] D. Tucker-Smith and N. Weiner, Phys. Rev. D 64 (2001) 043502.
- [100] C. R. Chen, Y. X. Lin, C. S. Nugroho, R. Ramos, Y. L. S. Tsai and T. C. Yuan, Phys. Rev. D 101 (2020) 035037.
- [101] H. Ishimori, T. Kobayashi, H. Ohki, H. Okada, Y. Shimizu, and M. Tanimoto, Prog. Theor. Phys. Suppl. **183**, 1 (2010).